Water sorption and diffusion in (reduced) graphene oxide-alginate biopolymer nanocomposites

Karolis Vilcinskas, Jure Zlopasa, Kaspar M.B. Jansen, Fokko M. Mulder, Stephen J. Picken, and Ger J. M. Koper*

Abstract. We analyze water sorption and diffusion in (reduced) graphene oxide-alginate composites of various compositions. Water sorption of Sodium alginate can be significantly reduced by the inclusion of graphene oxide sheets due to the formation of an extensive hydrogen-bonding network between oxygenated groups. Cross-linking alginate with divalent metal ions and presence of reduced graphene oxide can further improve the swelling resistance due to the strong interactions between metal ions, alginate and filler sheets. Depending on conditions and composition, overall water barrier properties of alginate composites improve upon (reduced) graphene oxide filling, making them attractive for moisture barrier coating applications.

Water sorption kinetics in all alginate composites indicate a non-Fickian diffusion process that can be accurately described by the Variable Surface Concentration model. In addition, water barrier properties of Sodium alginate-graphene oxide composites can be adequately predicted by using a simple model that takes orientational order of filler sheets and their effective aspect ratio into account.

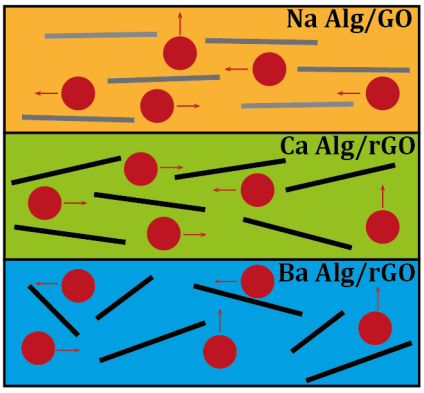

1. Introduction

It is well established that the presence of high aspect ratio filler platelets, i.e. platelets with a large size to thickness ratio, forces diffusing species to undertake longer pathways while traversing polymer composites, thereby significantly improving the composite's barrier properties [1]. As a consequence, polymer composites with completely exfoliated and regularly arranged filler platelets are desirable as barrier coatings [2]. Since their isolation in 2004 [3], graphene and its derivative graphene oxide have attracted enormous attention in the field of polymer composites [4]. In particular, the inherent gas impermeability of graphene [5] and graphene oxide [6] makes them attractive for the preparation of barrier composites [7]. Indeed, inclusion of graphene (oxide) has been shown to significantly reduce water permeability through poly(vinyl alcohol) [8], polyimide [9], different types of nylon [10], starch [11] and natural rubber [12] composites.

Recently, a few studies have addressed the properties of Sodium alginate-graphene oxide composites [13]. Alginate is a naturally occurring block copolymer, comprised of irregularly arranged blocks of β-D-mannuronic acid (M) and α-L-guluronic acid (G) that form cross-linked junctions with multivalent metal ions [14]. The hydrophilicity of Sodium alginate and the presence of oxygenated groups on graphene sheets enable the easy dispersion of graphene oxide in water. Hence, Sodium alginate-graphene oxide composites can be readily prepared by solution casting. Among other properties, one study [13b] has examined the swelling resistance and the pervaporation of ethanol/water mixtures for membranes of Sodium alginate-graphene oxide and Sodium alginate-reduced graphene oxide. The authors have shown that inclusion of graphene (oxide) improves the swelling resistance of composite films due to the presence of aligned graphene (oxide) sheets and the formation of a hydrogen-bonding network between oxygenated groups of graphene (oxide) and alginate chains. In

addition, the composite films exhibited a high selectivity and transport rate of water molecules due to the oxygen-containing groups on the graphene sheets, structural defects, edge-to-edge slits and interfacial free cavities. However, the authors of the study did not investigate the mechanism of water sorption and diffusion for their composite films.

Earlier studies by Andreopoulos [15] and Hirai et al. [16] examined water sorption and diffusion in Sodium alginate, alginic acid and Cobalt cross-linked alginate films. These authors observed sigmoidal shaped water sorption curves of different types of alginates that suggest a non-Fickian water diffusion mechanism in alginates. As yet, water sorption and diffusion in Sodium alginate-graphene (oxide) composites containing high weight fractions of filler as well as in divalent metal ions cross-linked alginate-reduced graphene oxide composites have not been investigated systematically.

In this study we explore water sorption of different alginates and their (reduced) graphene oxide composites. In addition, we model the diffusion mechanism in the composite films and quantify water mobility. Lastly, we will show that the water barrier properties of Sodium alginate-graphene oxide composites are related to the orientational order of graphene oxide sheets in alginate matrix and their effective aspect ratio.

This study is not only of purely academic interest. Biocompatibility of alginates [17] and good barrier properties of (reduced) graphene oxide could be attractive for barrier coating applications and its composites may find application in, for instance, the food industry [18].

2. Experimental section

2.1. Sample preparation

Sodium alginate salt (Protanal® RF 6650) was kindly provided by FMC Biopolymer. As stated by the manufacturer, guluronic to mannuronic acid ratio for this type of alginate was 1.5:1. To prepare 1 wt% aqueous polymer solution, 1 gram of Sodium alginate (Na-Alg) salt was dissolved in 99 grams demineralized water, containing 0.4 grams of glycerol (99+ Pure, Acros Organics) under vigorous stirring until a homogenous solution was attained.

Graphene oxide (GO) was prepared via Kovtyiukhova's method [19]. Composite films with various weight fractions of GO were prepared by drop-wise addition of an aqueous GO dispersion into a 1 wt% Na-Alg solution and continuously stirred until a visually homogenous mixture was attained. The mixture then was poured into a Petri dish and dried under vacuum at 50 °C overnight (about 15 h).

Subsequently, the thus obtained free-standing water-soluble Na-Alg/GO composite films of ~30 μm in thickness were cut into strips of about 30x3 mm^2 and immersed into a 5 wt% $CaCl_2$ (Sigma Aldrich) or a 5 wt% $BaCl_2 \cdot 2H_2O$ (Riedel-de Haën) solution for 20 min to obtain alkaline earth metal cross-linked alginate composite films. The excess salt was removed using copious amounts of demineralized water. The samples were dried under vacuum at 50 °C. Note that, without the cross-linking salt, the Na-Alg/GO films readily dissolve in water since they are hydrophilic, whereas the cross-linked films are water-insoluble and form a swollen gel.

Finally, the reduced graphene oxide (rGO)/alginate composite films were prepared by immersing the water-insoluble alkaline earth metal cross-linked alginate/GO composite films, as described above, into an aqueous hydrazine (Sigma Aldrich) solution for 48 h at ambient

temperature. The weight ratio of GO to hydrazine was about 10:7. During the course of reduction, the composite films changed their color appreciably, from dark brown to black. Hydrazine is not known to affect the alginate, therefore the color change indicates the reduction of GO to Gr. After reduction, the composite films were washed with demineralized water, dried under vacuum at 50 °C and stored in the desiccator with silica gel as the drying agent. Prior to further analysis, the samples were kept in the furnace at 50 °C under vacuum for at least 48 h. The microscopic structure of (reduced) graphene oxide-alginate composites is presented in the Supporting Information.

2.2. Characterization

Atomic force microscopy (NTMDT Ntegra) (AFM) was used to observe the morphology of graphene oxide sheets. For analysis, 0.05wt% graphene oxide aqueous dispersion was spin-coated on a clean silicon wafer (Siltronix) and examined in tapping mode.

Fourier Transform Infrared Spectroscopy (FTIR) experiments were performed with Nicolet 6700 spectrometer. The spectra were averaged over 128 scans at a resolution of 4 cm^{-1} in 650 – 4000 cm^{-1} range.

X-ray diffraction (XRD) measurements in Bragg-Brentano reflection mode were performed by a PANalytical X'Pert Pro PW3040/60 diffractometer with Cu Kα radiation operating at 45 kV and 40 mA in an angular 2θ range of 5°–50°.

Gravimetric water vapor sorption analysis (TGA-RH) was performed on a Q5000SA (TA Instruments) instrument at 20 °C and 60 °C in the 0 – 80 % relative humidity (RH) range. The instrument consists of a humidity and temperature-controlled chamber with inside a balance. Flushing the chamber with the combined streams of dry and wet nitrogen gas, the desired relative humidity values can be obtained where the installed thermocouples ensure

homogenous temperature in the chamber during the experiment. For each measurement, one piece of a rectangular sample was used that was visually inspected prior the measurement to be without any visible structural defects. The mass of all specimens was close to 2 mg.

For the measurements at 20 °C, the samples were initially equilibrated at 60 °C and 1% RH for 1 hour to ensure they were moisture-free. Afterwards the temperature was lowered to 20 °C and 1% RH, and the samples were allowed to equilibrate at the corresponding conditions for 1 hour. Subsequently, the temperature was kept constant at 20 °C and the RH values were increased by 20% in each step. Water mass uptake was measured for 200 min at each RH value. If the weight change was less than 2 μg for 10 min, the RH value was allowed to increase to a higher value. After having finished measuring the weight gain at 80% RH, the RH was lowered to 1%, and the desorption process continued for 800 min, unless the weight change was smaller than 2 μg for 10 min.

For the measurements at 60 °C, a similar procedure was followed in which the samples were subjected to pre-programmed relative humidity steps immediately after the drying step at 60 °C.

3. Results and discussion

3.1. FTIR analysis

There are strong indications in the literature [20] that alginate and its complex exhibit structural changes in the presence of multivalent ions. Hence, we included an FTIR analysis to analyze the influence of both filler material and multivalent ions, see Figure 1.

Figure 1

A summary of the characteristic peak positions is also presented in the Table 1. As recent studies [13c, 21] investigated Sodium alginate-graphene oxide composites spectra in detail, we only focus on spectra of divalent metal ion cross-linked-reduced graphene oxide composites and use the spectrum of Sodium alginate as a reference.

Table 1

As seen in Figure 1, the neat sodium alginate sample has produced characteristic peaks at 3305 cm^{-1}, 1607 cm^{-1}, 1410 cm^{-1}, 1090 cm^{-1} and 1030 cm^{-1}. The broad peak at 3305 cm^{-1} corresponds to stretching of hydroxyl groups, whereas the bands at 1607 cm^{-1} and 1410 cm^{-1} are characteristic for asymmetric stretching of carboxyl groups [20a]. The peak at 1030 cm^{-1} and a shoulder at 1090 cm^{-1} indicate stretching of C-O-C bonds [20b].

Since divalent metal ions can replace Sodium at carboxyl groups of alginate chains, the two peaks at 1607 cm^{-1} and 1410 cm^{-1} should be monitored for the ion exchange reaction [20a]. As presented in Figure 1A and Table 1, after cross-linking alginate with Ca^{2+} ions, the peak at 1607 cm^{-1} has significantly weakened, broadened and shifted to 1593 cm^{-1}. Furthermore, the peak at 1410 cm^{-1} has also weakened, expanded and shifted to 1418 cm^{-1}. In addition, the shoulder at 1090 cm^{-1} has disappeared, and the peaks at 3305 cm^{-1} and 1030 cm^{-1} weakened, broadened and shifted towards lower frequencies. These changes indicate substitution of

Sodium ions and formation of cross-linked egg-box junctions between Calcium ions, carboxyl groups and oxygen atoms of alginates, see [22] for a schematic illustration.

Upon inclusion of chemically reduced graphene oxide (rGO), the bands at 3275 cm^{-1}, 1593 cm^{-1} and 1022 cm^{-1} have continued to move to lower wavenumbers, and their intensity has slightly decreased, albeit not so for the band of asymmetric stretching of carboxyl group. Such changes suggest that upon inclusion of filler, the remaining unreduced oxygenated groups of rGO sheets can interact with the oxygenated groups of alginate chains, presumably via hydrogen-bonding. Indeed, during the hydrazine reduction process at ambient conditions, some of the oxygeneated groups, such as hydroxyl and/or carbonyl, are preserved [23]. A band at 2362 cm^{-1} is ascribed to CO_2 molecules present in the ambient.

Similar changes in spectra have been observed upon cross-linking with Barium ions, see Figure 1B, and subsequent inclusion of rGO, although with some differences. As for the Calcium cross-linked alginate, upon ion exchange reaction with Barium ions, the bands at 3305 cm^{-1}, 1607 cm^{-1} and 1410 cm^{-1} diminish in intensity and shift towards lower wavenumbers. However, the peak at 1030 cm^{-1} has moved to much lower frequency in comparison to that of Calcium alginate, and the shoulder at 1090 cm^{-1} has not disappeared, but rather shifts to lower wavenumbers. Such dissimilar interaction with divalent metal ions could presumably originate from the distinct binding of these ions to alginate chains [24] that we futher discuss in the succeeding paragraphs. In addition, these observations also suggest that Barium ions interact stronger with the oxygenated groups of alginate chains as manifested in the shift to lower frequencies. Upon inclusion of rGO, the characteristic peaks at 1577 cm^{-1}, 1397 cm^{-1} and 989 cm^{-1} do not change their position, but rather gradually diminish in intensity, whereas the shoulder peak only disappears for higher weight fractions of rGO. Such dissimilar interactions with Barium ions imply specific interactions between

different divalent metal ions, polymer and filler, that are governed by the affinity of metal ion to the polymer matrix and filler sheets.

3.2. Water sorption

Figure 2

Figure 2 (A)-(C) shows water sorption isotherms at 20°C for alginate composites of various compositions. Based on the classification of sorption isotherms proposed by Brunauer et al. [25], water sorption isotherms of Sodium alginate-graphene oxide (Na-Alg/GO) composites appear to possess a sigmoidal shape, often observed for hydrophilic polymers [26]. On the other hand, the water sorption isotherms of divalent metal ion cross-linked alginate-reduced graphene oxide composites are more characteristic to those of less hydrophilic polymers [27]. Indeed, the interaction of divalent metal ions with oxygenated groups of alginate significantly reduces water sorption capacity, which is further lowered by the more hydrophobic nature of chemically reduced graphene oxide. Although there are numerous water sorption models reported in literature[28], we have unfortunately not been able to obtain adequate fit of our data to any of them.

As illustrated in Figure 2 (A), the water uptake for Na-Alg/GO composites decreases with increasing weight fraction of graphene oxide (GO), most notably at higher water activity values a_w. However, the inclusion of small amounts (1 wt%) of GO slightly increases the water sorption capacity. We would like to point out that our composite films contain nearly 30 wt% of glycerol (by polymer weight) as a plasticizer that is known to strongly influence the water sorption capacity [29]. We suggest that upon addition of a small amount of GO, the initial hydrogen-bonding network between hydroxyl groups of glycerol and oxygenated groups of the alginate backbone is disrupted in a manner that allows more adsorption sites for the water molecules, hence increasing the sorption capacity. With further increment of the

GO weight fraction, favorable structural rearrangements take place that yield fewer adsorption sites for water molecules due to the formation of the extensive hydrogen-bonding network between oxygenated groups of GO sheets and polymer backbone [13c]. Furthermore, the water sorption capacity is also influenced by water activity. At low humidity values, sorption is insignificant due to the presence of a strong hydrogen-bonding network, but as the water activity increases, water uptake becomes more considerable due to the increased number of sorbed water molecules that weaken the hydrogen-bonding network between the filler sheets and alginate chains, thus increasing polymer chain mobility and free volume.

On the other hand, as illustrated in the Figure 2 (B)-(C), the water sorption capacity for divalent metal ion cross-linked alginate composites is significantly reduced, albeit not at low water activity (a_w=0.2) where it is higher than that of Na-Alg/GO composites. We propose that the higher water sorption capacity at low water activity arises due to the increased free volume in composites upon introduction of divalent metal ions. As initially available vacancies are occupied by water molecules, the improved swelling resistance at higher water activities can be attributed to strong interactions between divalent metal ions, oxygenated groups of graphene sheets and polymer backbone that solvent molecules are not able to break efficiently. In addition, Barium alginate composites show the lowest water sorption capacity, suggesting that the higher affinity of Ba^{2+} ions to the polymer backbone [30] and carboxyl groups present on the graphene oxide sheets [31] results in stronger interaction that significantly reduce water uptake in comparison to Calcium alginate and its composites. Indeed, interactions between divalent metal ion cross-linked alginates and their reduced graphene oxide composites, as analyzed by FTIR, have shown to be dependent on the divalent metal ion. Overall, the swelling resistance of alginate significantly improves upon introduction of cross-linked junctions with divalent metal ions. The strong interactions between divalent metal ions, oxygenated groups on graphene sheets, and the alginate backbone, as well as the

hydrophobic nature of reduced graphene oxide contribute to the decreased water sorption capacity.

Although not yet at equilibrium, Sodium alginate-graphene oxide composites appear to desorb almost completely whereas divalent metal ion cross-linked alginate-reduced graphene oxide composites still contain a small amount of water. This observation indicates that water molecules remain stronger bonded to the metal cross-linked alginate composites, presumably due to the higher coordination number of divalent metal ions [32].

Figure 3

As illustrated in Figure 3(A)-(C), the water sorption capacity of alginate composites at 60°C, is reduced. Water mass uptake of non-cross-linked Na-Alg/GO composites exhibit a negative slope, indicating dominance of desorption primarily whereas water sorption curves of divalent metal ion cross-linked alginate-graphene composites suggest prevailing water sorption process. Nonetheless, overall sorption capacity of alginate composites is reduced in comparison with that at 20°C. Such dissimilar behavior could arise from different interaction strength between the constituents in the cross-linked and non-cross-linked alginate composites. We speculate that the hydrogen-bonding network between oxygenated groups of graphene oxide and alginate backbone is being disrupted at elevated temperatures leading to substantial increase in free volume of the composites. Furthermore, interaction between water molecules and exposed oxygenated groups of the constituents are not strong enough to retain them attached by hydrogen bonding. Therefore, initially sorbed water molecules are only weakly bonded and able to escape via passages created by de-bonding between filler and polymer. In the divalent metal ion cross-linked alginate-reduced graphene oxide composites, however, bonding is primarily based on Coulombic interactions that are at least several times stronger than hydrogen-bonding [33]. Although some structural rearrangements occurring at

elevated temperatures should not be excluded, water molecules presumably are not able to attach to oxygenated groups of the constituents, therefore are able to move through interstitial cavities in the cross-linked alginate – graphene composites.

The peaks at high water activity (a_w=0.8) at 60°C are of experimental origin and should not be interpreted as real physical effects.

Figure 4

At the same time, the presence of plasticizer (glycerol) in the alginate composites should not be neglected. Our introductory analysis of water uptake of Sodium alginate containing various weight fractions of glycerol suggests an important role of glycerol. As presented in Figure 4, the presence of glycerol significantly affects the water sorption capacity of Sodium alginate. As seen in Figure 4 (A)-(B) at small weight fractions of glycerol, the water sorption capacity slightly decreases suggesting strong hydrogen-bonding based interaction between oxygenated groups of alginate and hydroxyl groups of glycerol, that water molecules are only able to disrupt at higher water activities. At higher weight fractions of plasticizer the water sorption presumably increases due to the excess of glycerol, where its hydrophilic groups offer binding sites for water molecules. Avella et al. [34] has investigated physico-mechanical properties of alginates comprised of dissimilar guluronic and mannuronic acid contents that contained varying weight fractions of glycerol. Having observed different thermal properties of alginates that showed strong plasticizer dependence, the authors suggested that binding of glycerol molecules to alginate chains is influenced by its weight fraction and the composition of the alginates. Namely, polymer chains of alginates rich in mannuronic acid units are more flexible and assume a more linear conformation, therefore glycerol molecules bonded to the polymer backbone still remain available. On the other hand, polymer chains of alginates rich in guluronic acid units are more folded and buckled, hence at low weight fractions of

glycerol, alginate chains can encase the glycerol molecules. At higher weight fractions of glycerol, the accessible binding sites to guluronic acid units become saturated, thus glycerol molecules bonded to mannuronic acid units offer adsorption sites to water molecules. Indeed, as seen in Figure 4 (A)-(B), for the higher guluronic acid content possessing alginate we have used in our experiments, water sorption increased at high weight fractions of glycerol.

3.3. Modeling water diffusion and structural changes in alginate composites

Figure 5

Figure 5 illustrates representative moisture sorption data (open symbols). All moisture sorption curves of alginate composites show a distinctive sigmoidal shape, indicating a non-Fickian water vapor diffusion mechanism in the composite films, previously also observed for alginate films [15-16]. In an attempt to model and quantify water diffusion in alginates and their composites, we have used the Variable Surface Concentration Model [35] to fit the experimental data (solid lines). In this model water sorption and diffusion take place in two steps. Initially, upon introduction of diffusing species, their concentration at the sample surface quickly jumps to a value C_0, and the diffusion process is governed by the concentration gradient established by C_0. In the second stage, the concentration of diffusing species slowly increases to equilibrium value of C_∞ via a first order relaxation process with relaxation rate k. As proposed by the authors, the concentration gradient in the second stage becomes negligibly small and the diffusion process is governed only by the increment of the surface concentration.

The relative mass uptake of diffusing species is expressed as [36]:

$$\frac{M_t}{M_\infty} = \phi\left[1 - \frac{8}{\pi^2}\sum_{n=0}^{\infty}\frac{\exp\left(\frac{-(2n+1)^2\pi^2\theta}{4}\right)}{(2n+1)^2}\right] + \left(1-\phi\right)\left[1 - \frac{\tan\sqrt{\psi}\exp(-\psi\theta)}{\sqrt{\psi}} - \frac{8}{\pi^2}\sum_{n=0}^{\infty}\frac{\exp\left(\frac{-(2n+1)^2\pi^2\theta}{4}\right)}{(2n+1)^2\left(1-\frac{(2n+1)^2\pi^2}{4\psi}\right)}\right] \quad (1)$$

The first term of Equation (2) represents the Fickian diffusion stage, where the diffusing species penetrate the sample due to the established concentration gradient. The second term of Equation (2) describes the diffusion process governed by the time-dependent surface concentration. In addition, Equation (2) contains three physically meaningful transport parameters, namely Φ – the relative initial concentration; D – the diffusion coefficient; ψ – the inverse of the diffusion Deborah number:

$$\phi = \frac{C_0}{C_\infty};\ \theta = \frac{Dt}{l^2};\ \psi = \frac{kl^2}{D} \tag{2}$$

where: C_0 is the initial water vapor concentration at the surface of the film sample; C_∞ – equilibrium water vapor concentration; k – relaxation rate; Θ – dimensionless time; t – sorption time, l – thickness of the film sample. A similar expression for the diffusion of solvent in polymer particles was studied by one of us [37].

The relative initial concentration Φ represents the ratio of the initial surface concentration of diffusing species to that achieved in the second stage of sorption. The dimensionless time Θ obtained from the fit of the model to the data enable the extraction of the diffusion coefficient D. The third parameter, the inverse of the diffusion Deborah number ψ, stems from the diffusion Deborah number [38], which is defined as the ratio of characteristic relaxation time of polymer chains versus the characteristic time of diffusion. The diffusion Deborah number is widely used for identification of non-Fickian diffusion effects [27]. When the diffusion Deborah number is significantly larger than unity, the reorganization of polymer chains is slow and the diffusion process occurs quickly, such that the whole process resembles that of diffusing species through a solid material. Similarly, if the conformational changes are quicker than the characteristic diffusion time, the diffusion Deborah number is significantly smaller than unity, and the Fickian diffusion process prevails. On the other hand, if both processes are on a

similar time scale, the diffusion and relaxation are coupled, and non-Fickian diffusion dominates, see references [38-39] for a comprehensive discussion.

As illustrated in Figure 5, there is excellent agreement between the experimental data (open symbols) and the Variable Surface Concentration Model (solid lines). Therefore, we used it to determine the relative initial concentration, the diffusion coefficient, and the diffusion Deborah number values for the alginate composites equilibrated at different temperatures and water activities.

3.3.1. Sodium alginate – graphene oxide composites

Figure 6

As seen in Figure 6 (A)-(B) with increasing amount of graphene oxide, the mobility of water molecules becomes impeded due to the increased diffusion path in the presence of obstacles for diffusing species [1]. In addition, at lower water activities the diffusion coefficient values are small and increase with increasing relative humidity, albeit with some exceptions. At 20°C and low water activity (a_w=0.2), the mobility of water molecules in guluronic acid units rich Sodium alginate containing ~30 wt% of glycerol is low due to the bulk encapsulation of glycerol molecules that apparently only slightly increase the unoccupied interstitial space between polymer chains available for water transport. As water activity increases, it begins to disrupt the hydrogen-bonding network between polymer and plasticizer, and adsorbed water molecules considerably increase the spacing between adjacent chains, thus allowing more room for solvent molecules to move. However, at high water activity (a_w=0.8), maneuverability of water molecules may become restricted due to lower mobility of water clusters [40]. As proposed by the author, at low water activities, the water molecules strongly attach to the available hydrophilic groups, thus becoming relatively immobile. As water activity increases, the hydrophilic groups become saturated and additional water molecules will bind more weakly to the already adsorbed water molecules, in this way forming a multilayer of water that is more mobile. With the further increment of water activity, the formation of water clusters results in decreased water mobility due to the relative immobility of these clusters.

Upon inclusion of graphene oxide sheets, water mobility does not change significantly at low water activity (a_w=0.2) and 20°C. As discussed earlier, the presence of an extensive and robust hydrogen-bonding network between oxygenated groups on graphene sheets and

alginate backbone offers few adsorption sites for molecules resulting in negligible amount of sorbed water. Therefore, the available adsorption sites strongly interact with attached water molecules and restrict their mobility. With increasing water activity, however, the water mobility in the composites improves due to the increased free volume caused by the sorption as well as higher mobility of the newly sorbed water molecules. On the other hand, high weight fractions of filler are effective in impeding water mobility, as the water molecules are compelled to take longer pathways due to the presence of GO sheets. The decreased water transport for the sample containing 1 wt% of GO at high water activity (a_w=0.8) corroborates water sorption results discussed in the preceding paragraph and illustrated in the Figure 2 (B), namely that increased water sorption capacity facilitates formation of relatively immobile water clusters.

In contrast to reports in literature [6, 13b], we have not observed reduced water barrier properties for Sodium alginate-graphene oxide composites. It has been argued that water molecules permeate through GO membranes entirely unimpeded due to the formation of empty spaces between non-oxidized regions of GO sheets that easily accommodate a monolayer of water molecules and allow low-frictional flow of them [6]. In addition, Cao et al. [13b] upon examination of sodium alginate-GO composites by Positron Annihilation Lifetime Spectroscopy, has concluded that addition of GO increases free volume in the sodium alginate-GO interface. Our data suggests that, even if transport of water molecules is unimpeded in GO sheets and the presence of additional space at the polymer-filler interface, inclusion of GO can nevertheless improve water barrier properties of Na-Alg/GO composites. Besides, 2 dimensional X-ray diffraction analysis of Na-Alg/GO composites reveals a high in-plane alignment of GO sheets [41] that should significantly enhance barrier properties in the direction along the layer normal of composite samples. We have attempted to estimate the

improvement of water barrier properties by taking into account the degree of filler alignment for Na-Alg/GO composites in the following paragraph.

Due to the increased kinetic energy of water molecules, water barrier properties at 60°C is significantly reduced in Sodium alginate-graphene oxide composites. Nonetheless, water barrier properties of the composites improve with the increasing weight fraction of GO sheets. Likewise for unfilled Sodium alginate and its 1 wt% GO composite at 20°C, the water mobility at 60°C initially increases with water activity, and is hindered at high water activity (a_w=0.8) due to the establishment of water clusters as discussed earlier. The samples containing higher weight fractions of GO show variable water activity dependence on mobility of solvent molecules. We speculate that increase in temperature disrupts the hydrogen-bonding network between polymer and plasticizer as well as polymer and filler, thereby offering adsorption sites for water molecules, which in turn initiates the earlier discussed diffusion mechanism.

Figure 7

Values of diffusion Deborah number in Sodium alginate-graphene oxide samples at various water activities at different temperatures are presented in Figure 7. As seen, the values are comparable and close to 2.5 for all the composites at all water activities at 20°C. Such close to unity value indicates that both relaxation and diffusion processes occur simultaneously. However, the diffusion Deborah number values at a_w= 0.2-0.4 are slightly higher for the composites containing 25 wt% of GO, implying that the extensive hydrogen-bonding network can restrict conformational changes. In addition, the diffusion Deborah number values at a_w=0.8 for unfilled Sodium alginate and its 1 wt% GO composite are also augmented, signifying the obstructive role of abundant water molecules to arrangements of polymer chains. The relative initial concentration values for all the samples are close to unity

(Φ = 0.99), suggesting that water vapor concentration at the samples surface has not changed significantly in the second stage of sorption.

3.3.2. Alkaline earth metal ion cross-linked alginates

Figure 8

Figure 8 (A)-(B) illustrate the water mobility in Calcium alginate-reduced graphene oxide (Ca-Alg/rGO) composites of various compositions at different temperatures and water activities. In contrast to unfilled Sodium alginate, the water mobility at 20°C in a Calcium alginate polymer matrix monotonically increases with the increasing water activity. Although water molecules diffuse faster at low water activities (a_w=0.2-0.4) in a Calcium alginate polymer matrix, their mobility is reduced at higher water activities (a_w=0.6-0.8), compared to unfilled Sodium alginate. Upon inclusion of 1 wt% of rGO, the water mobility in Calcium alginate-reduced graphene oxide composites is impeded at the investigated water activities range. In the samples containing higher weight fractions of rGO, water transport improves with increasing weight fraction of filler, and eventually becomes comparable to that of neat Calcium alginate for the samples containing 25 wt% of rGO. These observations suggest that the introduction of Ca^{2+} ions increases the free volume of polymer providing additional space for water molecules to move. Furthermore, inclusion of rGO appears to significantly alter the polymer structure when cross-linked with Calcium ions. We propose that upon cross-linking alginate with Calcium ions, the additional unoccupied space is created due to conformational changes of the polymer backbone. It has been reported that divalent metal ions, such as Calcium and Barium, have preferential binding sites to alginate oxygenated groups [24]. In their study the authors have suggested that Calcium ions preferentially bind to guluronic-guluronic acid and guluronic-mannuronic acid blocks. In particular, the presence of Calcium ions in between two guluronic acid units should increase the space between two adjacent polymer

chains, while specific binding of Calcium ions to guluronic-mannuronic acid blocks is believed to maintain the initially linear polymer chain conformation (see the schematic illustration in the cited article). Thus, at low water activities, water mobility is higher due to the created additional space when cross-linked junctions are formed. As seen in Figure 2 (C)-(D), the introduction of Calcium ions significantly improves the swelling resistance of the polymer, indicating a strong interaction between the metal ions and oxygenated groups of alginate chains that water molecules are not able to break efficiently even at high water activity values. Therefore, the formation of relatively immobile water clusters at high water activities in the available interstitial space reduces the diffusion coefficient value.

Presence of rGO in the Calcium alginate matrix, however, should inevitably alter the polymer structure. Before beginning to discuss effects of graphene weight fraction, we would like to reiterate that we conduct the ion exchange reaction of free-standing Na-Alg/GO composite films cut in stripes by immersing them into solution of divalent metal ion salt, and subsequently reducing metal ion cross-linked alginate/GO samples in an aqueous hydrazine solution. We have previously suggested that during these processes, the competing interactions between metal ions, polymer chains and filler sheets can initiate complex structural changes [41]. In addition, it has been reported [42] that Calcium ions readily interact with carboxylic groups that are present on the edges GO sheets. Thus, before reduction of the oxygenated groups on GO sheets, the following interactions may occur: Calcium ion-alginate, alginate-Calcium ion-graphene oxide and graphene oxide-Calcium ion-graphene oxide. Based on this information, we propose that upon inclusion of low and moderate fractions (≤ 15wt%) of rGO, the interactions between the metal ions, filler sheets and polymer chains results in structural arrangements that reduce free volume, possibly by favorable Calcium ion-alginate and alginate-Calcium ion-reduced graphene oxide interactions, thus restricting water mobility and water sorption capacity (Figure 1 D). In

addition, scarcity of oxygenated groups on rGO sheets that have been eliminated after reduction offer few sorption sites for water molecules. With further increment of rGO content, the competing interactions between the constituents presumably promotes the formation of interstitial cavities that ease transport of water molecules in the composite samples containing ≥15 wt% of rGO.

At increased temperatures the mobility of water molecules increases, as illustrated in Figure 5B. Most notably, the transport of solvent molecules significantly increases for unfilled Calcium alginate, whereas its composites with rGO show diminished diffusion coefficient values. Such observations suggest that the onset of hydro-thermally assisted decross-linking/bond re-arrangement, especially when $a_w \geq 0.6$, could be responsible for the improved water mobility in neat Calcium alginate. On the other hand, addition of rGO appears to favorably alter hydro-thermally induced structural re-arrangements in a complex manner that improves water barrier properties of Calcium alginate composites at higher temperatures.

Figure 9

Estimated values of diffusion Deborah number in Ca-Alg/rGO composites at various water activities and temperatures are presented in the Figure 9. In contrast to non-cross-linked Na-Alg/GO composites, the values of the parameter vary significantly with composition and water activity. Nonetheless, the values lie in between 1-10, indicating that concurrent diffusion and relaxation processes are taking place. Compared to the values of the diffusion Deborah number in unfilled Sodium alginate, the values of the corresponding parameter in Calcium alginate are slightly increased, suggesting reduced polymer chain mobility upon introduction of cross-linked junctions with Calcium ions. Upon inclusion of rGO in the Calcium alginate matrix, the diffusion Deborah number values change in a complicated manner, suggest complex multiple interactions between the constituents of the composites. In

comparison to the non-cross-linked Na-Alg/GO composites, the equilibrium ratio constant Φ values for the Ca-Alg/rGO composites have decreased and lied in between 0.85-0.98, depending on water activity and composition. The highest values of Φ have been obtained for the samples at low water activity (a_w=0.2), which gradually decreased with increasing water activity. Such changes suggest that cross-linking alginate with Calcium ions and presence of rGO increases hydrophobicity of the polymer and its composites.

As for the diffusion Deborah number values at 60°C in Calcium alginate and its rGO composites, it appears that increasing water activity significantly improves polymer chain mobility as manifested in the decreasing diffusion Deborah number values. However, the uncertain variation of this parameter with the weight fraction of rGO suggests complex hydro-thermally induced interactions taking place in Calcium alginate and its rGO composites. The relative initial concentration Φ values for the composites exhibit similar values to that observed for the samples at 20°C.

Figure 10

Figure 10 (A)-(B) illustrate water transport in Barium alginate-reduced graphene oxide (Ba-Alg/rGO) composites of various compositions at different temperatures and water activities. In comparison to unfilled Calcium alginate, the water mobility at 20°C in Barium alginate decreases, except at water activity a_w=0.2. In addition, the water diffusion coefficient values in Barium cross-linked alginate remain lower at higher water activities (a_w=0.6-0.8) in comparison to non-cross-linked Sodium alginate. Contrary to Ca-Alg/rGO composites, inclusion of rGO promotes water mobility in Ba-Alg/rGO composites, albeit not in the samples containing 25 wt% of rGO. Depending on the composition and water activity, transport of water molecules is enhanced in Ba-Alg/rGO composites compared to Ca-Alg/rGO and Na-Alg/GO composites.

As introduced earlier, divalent metal ions show different binding affinity to mannuronic and guluronic acid blocks that comprise alginates [24]. As suggested by the authors, Barium ions exclusively bind to two guluronic acid and/or two mannuronic acid blocks (see the schematic illustration at the cited article). Such preferential binding of Barium ions renders a different alginate chain conformation compared to Calcium alginate. The presence of bigger Barium ions between two guluronic acid units should contribute to the increased free volume. On the other hand, binding to two mannuronic acid block of neighboring chains could compensate for the increased free volume. In addition, Barium ions possess higher affinity to the alginate matrix, hence binding to the oxygenated groups occurs more readily [30]. As revealed by X-ray diffractograms, the higher affinity of Barium ions and the preferential binding to alginate building blocks result in a semi-crystalline structure of Barium alginate, whereas Sodium and Calcium alginate possess an amorphous structure [41]. Based on this information, we propose that binding of Barium ions to mannuronic acid units flattens out the alginate chains thereby allowing mannuronic acid blocks to assume a linear conformation and order parallel to each other. In addition, X-ray diffraction studies of Barium alginate-reduced graphene oxide composites revealed a structural evolution, suggesting the formation of a quasi-crystalline structure upon addition of graphene [41]. We speculate that in Ba-Alg/rGO composites, alginate-Barium ion-alginate, and reduced graphene oxide-Barium ion-reduced graphene oxide interactions prevail as suggested by the observed X-ray diffractions patterns and the higher affinity of Barium ions to alginate [30] and graphene[31]. Such preferential interactions could result in conformational changes that increase unoccupied space in the composites, hence, allowing increased water mobility. On the other hand, at high weight fractions of rGO (≥25wt%), as discussed earlier, competing reactions between the constituents and higher affinity of Barium ions both to polymer and filler could promote structural changes that reduce the free volume which results in a reduced water mobility in the samples containing

25 wt% of rGO. However, further studies invoking Positron Annihilation Lifetime Spectroscopy are required to verify the raised hypotheses for divalent metal ion cross-linked alginates and their reduced graphene oxide composites.

Likewise for other alginate composite systems, the increase in temperature facilitates water mobility in Ba-Alg/rGO composites. However, of all investigated alginate composite systems, transport of solvent molecules in Ba-Alg/rGO composites reveal the highest complexity. Contrary to previous observations, water diffusion coefficient values in Barium cross-linked composites show a tendency to decrease with increasing water activity. At present we cannot offer a sensible explanation for this effect.

Figure 11

.The values for the diffusion Deborah number for Ba-Alg/rGO composites at different temperatures and water activities are presented in Figure 11. Likewise to Calcium alginate, the values at 20°C for Barium alginate are higher than those for Sodium alginate. Furthermore, the values are higher than those of Calcium alginate, indicating that higher affinity of Barium ions to alginate reduces polymer chain mobility more. As for the diffusion Deborah number values in Ba-Alg/rGO composites, they are comparable with those in Ca-Alg/rGO composites, and also exhibit a complex variation with water activities and composition. The initial relative concentration Φ values have shown similar values to that observed for Ca-Alg/rGO composites, thus suggesting improved hydrophobicity of Ba-Alg/rGO composites.

The diffusion Deborah number values in Ba-Alg/rGO composites at 60°C show a similar trend as Ca-Alg/rGO composites with increasing water activities. However, the complex multiple parameter fitting procedure as well as at present undetermined hydro-thermally induced structural changes that take place precludes further discussion.

3.4. Modeling water barrier properties in Sodium alginate – graphene oxide composites

Having estimated the water mobility in Na-Alg/GO composites by using the Variable Surface Concentration model, we have attempted to describe the enhancement of the water vapor barrier properties in the composites at 20°C and a_w=0.6 taking into account the orientational order of the graphene oxide sheets in the alginate matrix [41]. We have applied a model, first proposed by L.E. Nielsen [1], of regularly arranged impermeable platelets embedded in a polymer matrix. The model is based on the assumption that in the presence of evenly dispersed impermeable platelets, the diffusing species will be compelled to take longer and more tortuous pathways, resulting in a significant increase in diffusion time and improved barrier properties. The barrier properties in composites are primarily governed by the size of filler (aspect ratio) and its volume fraction. However, this model assumes perfectly aligned and homogenously distributed platelets that do not form agglomerates. In order to account for imperfectly aligned filler platelets, the original model has been modified by Bharadwaj [43] to include the average order parameter $<P_2>$ values [44]. For perfectly aligned inclusions the average order parameter $<P_2>$ =1, whereas for istropically oriented platelets $<P_2>$ =0. Based on the modified model, the relative diffusivity can be expressed as:

$$\frac{D}{D_0} = \frac{1-\phi_F}{1+\frac{\alpha}{2}\phi_F\left[\frac{2}{3}\left(\langle P_2\rangle+\frac{1}{2}\right)\right]} \tag{3}$$

where: D_0 is the diffusion coefficient in a polymer matrix, D – diffusion coefficient in a composite, Φ_F – filler volume fraction, α – aspect ratio of filler particles, $<P_2>$ - order parameter value.

We have recently observed highly aligned GO sheets within Sodium alginate matrix and quantified the average order parameter values $<P_2>$ for various filler weight fractions [41]. By employing Equation (3), we have tried to predict relative diffusivity in Sodium alginate – graphene oxide composites by assuming three different aspect ratios of graphene oxide sheets, and to compare the obtained values with the experimentally observed (see Figure 12 A).

Figure 12

As seen in Figure 12 (A), at high aspect ratio the presence of graphene oxide sheets ensure better water vapor barrier properties of the composite films (dotted, dashed and dashed-dotted lines in the Figure 12 (A)), however a single high aspect ratio value does not enable to accurately predict the experimentally observed values. As illustrated in the Figure 11 B, graphene oxide sheets deposited from a dilute solution possess the average aspect ratio of 1000, however we have observed stacking of sheets with increasing weight fraction of filler, which, in turn, would reduce the effective aspect ratio of graphene oxide sheets, especially at high weight fractions of filler. Therefore, we model water vapor barrier properties of the composites with varying aspect ratio of graphene oxide sheets. We suggest that at low volume fractions of filler, the aspect ratio remains high and close to 1000. With increasing weight fraction it gradually decreases until it becomes significantly smaller. Indeed, as illustrated in the Figure 12 (A) by solid line, such estimation gives an adequate description of the experimentally obtained diffusivity in Sodium alginate-graphene oxide composites. So, by assuming varying aspect ratio of filler sheets and their average orientational order, water vapor barrier properties can be adequately estimated by invoking modified Nielsen's model.

4. Conclusions

We have investigated water sorption and diffusion in different alginate bionanocomposites. The FTIR spectra of divalent metal ion cross-linked alginates reveal stronger interaction between Barium ions and alginate chains in comparison to Calcium ions due to the higher affinity of the former. Upon introduction of the filler, the interactions between the constituents of the composites quickly become too complex to study with the present methods.

From the exposed water sorption and solvent mobilities at different temperatures and water activities in cross-linked and non-cross-linked alginate (reduced) graphene oxide composites, the sorption isotherms, showing a sigmoidal shape indicating a non-Fickian solvent diffusion mechanism, could be derived. The obtained isotherms can be modeled by the Variable Surface Concentration model. We conclude that overall, depending on the composition, alginate-reduced graphene oxide composites can indeed effectively reduce water mobility and therefore become attractive to coating applications. Furthermore, water barrier properties of Sodium alginate-graphene oxide composites can be adequately predicted by invoking a modified Nielsen's model that takes into account average orientational order of filler sheets and their effective aspect ratio.

Supporting Information

X-ray scattering patterns of (A) Na-Alg/GO composite films, (B) Ca-Alg/rGO composite films, and (C) Ba-Alg/rGO composite films are presented in Figure S1.

Appendix/Nomenclature/Abbreviations

Acknowledgements.

This work is supported by NanoNextNL, a micro and nanotechnology consortium of the Government of the Netherlands and 130 partners. The authors acknowledge M.Bus for the help obtaining AFM images, K.Goubitz – for XRD measurements, and H.Broekhuizen – for assistance with the TGA-RH instrument.

Received: Month XX, XXXX; Revised: Month XX, XXXX; Published online:

((For PPP, use "Accepted: Month XX, XXXX" instead of "Published online")); DOI: 10.1002/marc.((insert number)) ((or ppap., mabi., macp., mame., mren., mats.))

Keywords: composites, alginates, graphene oxide, crosslinking, water diffusion

References

1. Nielsen, L. E. *Journal of Macromolecular Science: Part A - Chemistry* **1967,** *1* (5), 929-942.

2. Lange, J.; Wyser, Y. *Packag Technol Sci* **2003,** *16* (4), 149-158.

3. Novoselov, K. S.; Geim, A. K.; Morozov, S. V.; Jiang, D.; Zhang, Y.; Dubonos, S. V.; Grigorieva, I. V.; Firsov, A. A. *Science* **2004,** *306* (5696), 666-669.

4. (a) Compton, O. C.; Nguyen, S. T. *Small* **2010,** *6* (6), 711-723; (b) Huang, X.; Qi, X. Y.; Boey, F.; Zhang, H. *Chem Soc Rev* **2012,** *41* (2), 666-686; (c) Gambhir, S.; Jalili, R.; Officer, D. L.; Wallace, G. G. *Npg Asia Mater* **2015,** *7*.

5. Bunch, J. S.; Verbridge, S. S.; Alden, J. S.; van der Zande, A. M.; Parpia, J. M.; Craighead, H. G.; McEuen, P. L. *Nano Lett* **2008,** *8* (8), 2458-2462.

6. Nair, R. R.; Wu, H. A.; Jayaram, P. N.; Grigorieva, I. V.; Geim, A. K. *Science* **2012,** *335* (6067), 442-444.

7. Yoo, B. M.; Shin, H. J.; Yoon, H. W.; Park, H. B. *J Appl Polym Sci* **2014,** *131* (1).

8. Huang, H. D.; Ren, P. G.; Chen, J.; Zhang, W. Q.; Ji, X.; Li, Z. M. *J Membrane Sci* **2012,** *409*, 156-163.

9. Tseng, I. H.; Liao, Y. F.; Chiang, J. C.; Tsai, M. H. *Mater Chem Phys* **2012,** *136* (1), 247-253.

10. Jin, J.; Rafiq, R.; Gill, Y. Q.; Song, M. *Eur Polym J* **2013,** *49* (9), 2617-2626.

11. Ma, T. T.; Chang, P. R.; Zheng, P. W.; Ma, X. F. *Carbohyd Polym* **2013,** *94* (1), 63-70.

12. Yan, N.; Buonocore, G.; Lavorgna, M.; Kaciulis, S.; Balijepalli, S. K.; Zhan, Y. H.; Xia, H. S.; Ambrosio, L. *Compos Sci Technol* **2014,** *102*, 74-81.

13. (a) Ionita, M.; Pandele, M. A.; Iovu, H. *Carbohyd Polym* **2013,** *94* (1), 339-344; (b) Cao, K. T.; Jiang, Z. Y.; Zhao, J.; Zhao, C. H.; Gao, C. Y.; Pan, F. S.; Wang, B. Y.; Cao, X.

Z.; Yang, J. *J Membrane Sci* **2014,** *469*, 272-283; (c) Chen, K.; Shi, B.; Yue, Y. H.; Qi, J. J.; Guo, L. *Acs Nano* **2015,** *9* (8), 8165-8175.

14. *Advances in Natural Polymers: Composites and Nanocomposites*. 1 ed.; Springer-Verlag Berlin Heidelberg: 2013; Vol. 18, p 426.

15. Andreopoulos, A. G. *Biomaterials* **1987,** *8* (5), 397-400.

16. Hirai, A.; Odani, H. *J Polym Sci Pol Phys* **1994,** *32* (14), 2329-2337.

17. *Advances in Natural Polymers: Composites and Nanocomposites*. 1 ed.; Springer-Verlag Berlin Heidelberg: 2013; p 426.

18. Arora, A.; Padua, G. W. *J Food Sci* **2010,** *75* (1), R43-R49.

19. Kovtyukhova, N. I.; Ollivier, P. J.; Martin, B. R.; Mallouk, T. E.; Chizhik, S. A.; Buzaneva, E. V.; Gorchinskiy, A. D. *Chem Mater* **1999,** *11* (3), 771-778.

20. (a) Sartori, C.; Finch, D. S.; Ralph, B.; Gilding, K. *Polymer* **1997,** *38* (1), 43-51; (b) Li, J. W.; He, J. M.; Huang, Y. D.; Li, D. L.; Chen, X. T. *Carbohyd Polym* **2015,** *123*, 208-216.

21. Wei, N.; Peng, X. S.; Xu, Z. P. *Acs Appl Mater Inter* **2014,** *6* (8), 5877-5883.

22. *Polysaccharides and Polyamides in the Food Industry. Properties, Production, and Patents.* 2005; p 783.

23. Pei, S. F.; Cheng, H. M. *Carbon* **2012,** *50* (9), 3210-3228.

24. Paredes, J. G. A.; Spasojevic, M.; Faas, M. M.; de Vos, P. *Frontiers in Bioengineering and Biotechnology* **2014,** *2* (26), 1-15.

25. Brunauer, S.; Deming, L. S.; Deming, W. E.; Teller, E. *J Am Chem Soc* **1940,** *62*, 1723-1732.

26. Jonquieres, A.; Fane, A. *J Appl Polym Sci* **1998,** *67* (8), 1415-1430.

27. van der Wel, G. K.; Adan, O. C. G. *Prog Org Coat* **1999,** *37* (1-2), 1-14.

28. Basu, S.; Shivhare, U. S.; Mujumdar, A. S. *Dry Technol* **2006,** *24* (8), 917-930.

29. (a) Talja, R. A.; Helen, H.; Roos, Y. H.; Jouppila, K. *Carbohyd Polym* **2007,** *67* (3), 288-295; (b) Olivas, G. I.; Barbosa-Canovas, G. V. *Lwt-Food Sci Technol* **2008,** *41* (2), 359-366.

30. Haug, A.; Smidsrod, O. *Acta Chem Scand* **1970,** *24* (3), 843-&.

31. Sun, P. Z.; Zheng, F.; Zhu, M.; Song, Z. G.; Wang, K. L.; Zhong, M. L.; Wu, D. H.; Little, R. B.; Xu, Z. P.; Zhu, H. W. *Acs Nano* **2014,** *8* (1), 850-859.

32. Persson, I. *Pure Appl Chem* **2010,** *82* (10), 1901-1917.

33. Hu, K. S.; Kulkarni, D. D.; Choi, I.; Tsukruk, V. V. *Prog Polym Sci* **2014,** *39* (11), 1934-1972.

34. Avella, M.; Di Pace, E.; Immirzi, B.; Impallomeni, G.; Malinconico, M.; Santagata, G. *Carbohyd Polym* **2007,** *69* (3), 503-511.

35. Long, F. A.; Richman, D. *J Am Chem Soc* **1960,** *82* (3), 513-519.

36. Sun, Y. M. *Polymer* **1996,** *37* (17), 3921-3928.

37. van der Zeeuw, E. A.; Sagis, L. M. C.; Koper, G. J. M. *Macromolecules* **1996,** *29* (2), 801-803.

38. Vrentas, J. S.; Jarzebski, C. M.; Duda, J. L. *Aiche J* **1975,** *21* (5), 894-901.

39. Papanu, J. S.; Soane, D. S.; Bell, A. T.; Hess, D. W. *J Appl Polym Sci* **1989,** *38* (5), 859-885.

40. Park, G. S., Transport Principles—Solution, Diffusion and Permeation in Polymer Membranes. In *Synthetic Membranes: Science, Engineering and Applications*, Bungay, P. M.; Lonsdale, H. K.; de Pinho, M. N., Eds. Springer Netherlands: 1986; pp 57-107.

41. Vilcinskas, K.; Norder, B.; Goubitz, K.; Mulder, F. M.; Koper, G. J. M.; Picken, S. J. *Macromolecules* **2015,** *48* (22), 8323-8330.

42. Park, S.; Lee, K. S.; Bozoklu, G.; Cai, W.; Nguyen, S. T.; Ruoff', R. S. *Acs Nano* **2008,** *2* (3), 572-578.

43. Bharadwaj, R. K. *Macromolecules* **2001,** *34* (26), 9189-9192.

44. de Gennes, P. G.; Prost, J., *The Physics of Liquid Crystals*. Second Edition ed.; Oxford University Press: 1995; p 347.

Table 1. Summary of characteristic peaks of composites of various compositions, see Figure 1.

Composition		**Peak positions (cm^{-1})**				
Polymer	Filler wt%	O-H stretching	C-O-O$^-$ stretching	C-O-O$^-$ stretching	C-O-C stretching	C-O-C stretching
Na-Alg/GO	0	3305	1607	1410	1090	1030
Ca-Alg/rGO	0	3275	1593	1418	-	1021
	6.3	3190	1577	1418	-	1022
	11.8	3170	1558	1418	-	1017
	25.0	3170	1576	1418	-	1018
Ba-Alg/rGO	0	3179	1577	1397	1080	989
	6.3	3179	1577	1397	1080	989
	11.8	3178	1576	1397	1080	989
	25.0	3101	1558	1397	-	-